Redox Biology 58 (2022) 102558

Contents lists available at ScienceDirect

Redox Biology

journal homepage: www.elsevier.com/locate/redox

Small extracellular vesicles from *Ptpn1*-deficient macrophages alleviate intestinal inflammation by reprogramming macrophage polarization via lactadherin enrichment

Dandan Han [a], Dongdong Lu [a], Shimeng Huang [a], Jiaman Pang [a], Yujun Wu [a], Jie Hu [a], Xiangyu Zhang [a], Yu Pi [a], Guolong Zhang [b], Junjun Wang [a,*]

[a] State Key Laboratory of Animal Nutrition, College of Animal Science and Technology, China Agricultural University, Beijing, 100193, China
[b] Department of Animal and Food Sciences, Oklahoma State University, Stillwater, Oklahoma, 74078, USA

ARTICLE INFO

Keywords:
Intestinal inflammation
Macrophage reprogramming
Ptpn1
Small extracellular vesicles
Lactadherin

ABSTRACT

Tyrosine-protein phosphatase non-receptor type 1 (Ptpn1) is known to be involved in macrophage polarization. However, whether and how Ptpn1 regulates macrophage phenotype to affect intestinal epithelial barrier function remains largely unexplored. Herein, we investigated the impact of Ptpn1 and macrophage-derived small extracellular vesicles (sEVs) on macrophage-intestinal epithelial cell (IEC) interactions in the context of intestinal inflammation. We found that *Ptpn1* knockdown shifts macrophages toward the anti-inflammatory M2 phenotype, thereby promoting intestinal barrier integrity and suppressing inflammatory response in the macrophage-IEC co-culture model. We further revealed that conditioned medium or sEVs isolated from *Ptp1b* knockdown macrophages are the primary factor driving the beneficial outcomes. Consistently, administration of the sEVs from *Ptpn1*-knockdown macrophages reduced disease severity and ameliorated intestinal inflammation in LPS-challenged mice. Furthermore, depletion of macrophages in mice abrogated the protective effect of *Ptpn1*-knockdown macrophage sEVs against *Salmonella* Typhimurium infection. Importantly, we found lactadherin to be highly enriched in the sEVs of *Ptpn1*-knockdown macrophages. Administration of recombinant lactadherin alleviated intestinal inflammation and barrier dysfunction by inducing macrophage M2 polarization. Interestingly, sEVs lactadherin was also internalized by macrophages and IECs, leading to macrophage M2 polarization and enhanced intestinal barrier integrity. Mechanistically, the anti-inflammatory and barrier-enhancing effect of lactadherin was achieved by reducing TNF-α and NF-κB activation. Thus, we demonstrated that sEVs from *Ptpn1*-knockdown macrophages mediate the communication between IECs and macrophages through enrichment of lactadherin. The outcome could potentially lead to the development of novel therapies for intestinal inflammatory disorders.

1. Introduction

Intestinal epithelial cells (IECs) provide the first line of defence for the mucosal barrier against various invading pathogens, toxic luminal stimuli, and other immunogenic substances [1,2]. However, coordinated release of immune effector molecules by IECs often works in concert to recruit and activate various types of immune cells and amplify mucosal inflammatory response, resulting in intestinal barrier disruption [3]. The intestinal barrier defect subsequently facilitates microbial translocation to the submucosa that leads to exacerbated inflammation and cytokine storm [3,4]. Dynamic interactions among intestinal microorganisms, IECs, and local immune cells are not only essential for maintaining intestinal homeostasis and mounting protective immunity to pathogens, but also responsible for pathogenesis and development of inflammatory bowel disease (IBD) [4–6].

Intestinal macrophages constitute a central hub to initiate and orchestrate an effective immune response towards tolerance or inflammation in the intestinal tract [7,8]. Under normal physiological conditions, circulating monocytes gradually replenish and differentiate toward an interleukin (IL)-10-producing phenotype known as alternatively activated or M2 macrophages. When recruited to the intestine during intestinal inflammation, macrophages undergo

* Corresponding author. College of Animal Science and Technology, China Agricultural University, Beijing, 100193, China.
E-mail address: wangjj@cau.edu.cn (J. Wang).

https://doi.org/10.1016/j.redox.2022.102558
Received 7 October 2022; Received in revised form 22 November 2022; Accepted 26 November 2022
Available online 28 November 2022
2213-2317/© 2022 Published by Elsevier B.V. This is an open access article under the CC BY-NC-ND license (http://creativecommons.org/licenses/by-nc-nd/4.0/).

pro-inflammatory transcriptional reprogramming, switching to classically activated or M1 macrophages, which are characterized by producing inflammatory cytokines such as IL-6, IL-1β, and tumor necrosis factor (TNF)-α [9]. Recent studies have suggested that modulating macrophage phenotypes and functions may provide a potential therapeutic strategy to those disorders where macrophages are involved [10,11].

Tyrosine-protein phosphatase non-receptor type 1 (Ptpn1), also known as protein tyrosine phosphatase 1B (Ptp1b), is a negative regulator of the insulin signalling pathway and has been proposed as a promising drug target to treat over-nutrition and obesity-induced insulin resistance [12,13]. More recently, the role of Ptpn1 in developing chronic inflammatory disorders has been studied [14]. However, the results are paradoxical. Ptpn1 deficiency were reported to result in enhanced M1 macrophage polarization, exacerbated mucosal inflammation, and impaired intestinal barrier integrity [14–16]. However, inhibition of Ptpn1 was also known to promote M2 macrophage polarization and prevent excessive inflammation [17,18]. Therefore, the paradoxical role of Ptpn1 in regulating inflammatory response is likely context-dependent and dictated by the types of cells and diseases involved.

SEVss are membrane-bound vesicles secreted by most eukaryotic cells and are increasingly appreciated to mediate the cell-to-cell crosstalk [19,20]. They are shown to shuttle and coordinate cellular responses by transferring genetic information and other effector molecules from donor to recipient cells [21–24]. However, the role of small extracellular vesicles (sEVs) and their mode of action are still ill-defined during immune activation and inflammation. Therefore, the objective of this study was to investigate the role of Ptpn1 in macrophage polarization in the context of inflammation and whether sEVs could be explored to manipulate the outcome of intestinal inflammation.

2. Materials and methods

2.1. Cell culture and co-culture

RAW264.7 cells were cultured in DMEM supplemented with 10% heat-inactivated FBS and treated with 100 ng/mL LPS and 20 ng/mL IFN-γ for 48 h to induce M1 polarization or with 50 ng/mL IL-4 for 48 h to induce M2 polarization. Macrophages were then washed thoroughly and replenished with fresh complete DMEM for another 24 h before the conditioned medium were collected. Intestinal epithelial cell lines, IEC-6, MODE-K and IPEC-1, were cultured in DMEM with 10% FBS or 20% conditioned medium. For co-culture system, RAW264.7 cells were seeded in 12-well plates and cultured with IECs grown on permeable transwell inserts for 24 h before collecting the supernatants for subsequent assays as described below.

2.2. Cell viability and LDH release assay

Cell viability and LDH released in the supernatants of cell culture was measured with Cell Counting Kit-8 (CCK-8) solutions (Dojingdo Laboratories, Kumamoto, Japan) and LDH Assay Kit-WST® (Dojingdo Laboratories, Kumamoto, Japan), respectively, according to the manufacturer's instructions.

2.3. Intracellular ROS and iron assay

Intracellular ROS accumulation and iron concentration were measured with a ROS detection kit (Solarbio, Beijing, China) and an iron assay kit (Abcam, Cambridge, MA, USA), respectively, as recommended by each manufacturer.

2.4. ELISA

The cytokine levels in the mouse serum, intestinal tissue homogenates and cell culture supernatants were quantified using mouse TNF-α ELISA Set II (BD Biosciences), mouse IL-6 ELISA Kit (BD Biosciences), mouse IL-1β ELISA Flex Set (BD Biosciences), and mouse lactadherin Quantikine Kit (R&D Systems) according to the manufacturers' instructions.

2.5. RNA interference and RT-PCR

The siRNAs targeting mouse *Ptpn1* and scrambled siRNAs were synthesized and transfected into RAW264.7 cells using Lipofectamine™ RNAiMAX (Invitrogen, USA) according to the manufacturer's instruction. Total RNA was extracted with TRIzol reagent (TransGen, Beijing, China) and converted to cDNA using iScript first-strand cDNA synthesis kit (TransGen, Beijing, China). Real-time PCR was performed using SYBR Green on ABI ViiATM 7 Real-Time System (Thermo Fisher Scientific). Threshold cycle numbers were normalized to housekeeping genes (*β-actin* and *Gapdh*). Primer sequences are shown as Supplementary Table 2.

2.6. Small extracellular vesicles isolation and identification

Small extracellular vesicles were collected from the conditioned medium, centrifuged, and concentrated using 100-kDa molecular weight centrifugal filters (Millipore) at 4000×*g* for 20 min as described [22]. Conditioned cell culture medium was centrifuged sequentially at 4000×*g* for 30 min and 8000×*g* for 1 h to remove large and small particles, followed by ultracentrifugation at 110 000×*g* for 2 h at 4 °C to pellet the sEVs. The pellet was washed once, resuspended in sterile PBS or culture medium, and stored at −80 °C until use. Nanosight (Malvern, Malvern, UK) analysis and transmission electron microscopy (TEM) (JEOL JMPEG- PTMC-1230, Japan) were used to identify sEVs. Markers of sEVs including CD63, and annexin A1 were analyzed by Western blot.

2.7. Cellular uptake of small extracellular vesicles

Small extracellular vesicles were stained with DiI (1,1′ -dioctadecyl-3,3,3′, 3′ -tetramethylindocarbocyanine perchlorate; Sigma), a lipophilic fluorescent dye, and incubated with IEC-6 or macrophages that were cultured on 6-well slides for 6 or 12 h, respectively. Cell culture medium was changed to Hank's balanced salt solution (HBSS) 15 min before being exposed to DiI-labelled sEVs. DiI-positive cells were analyzed using confocal microscopy.

2.8. Mass spectrometry

WT-macrophage and *Ptp1b* KD-derived macrophage sEVs (10 μg protein/sample) in PBS were analyzed in duplicate by reversed phase nano-LC-MS/MS (EASY-nLC coupled to Q Exactive Plus, Thermo Fisher Scientific) as previously described [22]. Data obtained were analyzed using Proteome Discoverer workflow (Thermo Fisher Scientific) against the UniProt database using the following parameters: maximum number of missed cleavages, 2; precursor tolerance, 20 ppm; dynamic modification, oxidation (M) and N-terminal protein acetylation, deamidated (NQ); static modification, carbamidomethyl (C); and false discovery rate, <0.01.

2.9. Western blotting

Small extracellular vesicles were lysed and subjected to sodium dodecyl sulphate polyacrylamide gel electrophoresis (SDS-PAGE) prior to transfer to PVDF membranes. After blocking with 5% (w/v) BSA, membranes were probed with specific primary antibodies at 4 °C overnight, followed by corresponding HRP-conjugated secondary antibodies. The bands were detected using an enhanced chemiluminescence kit (Solarbio, Beijing, China).

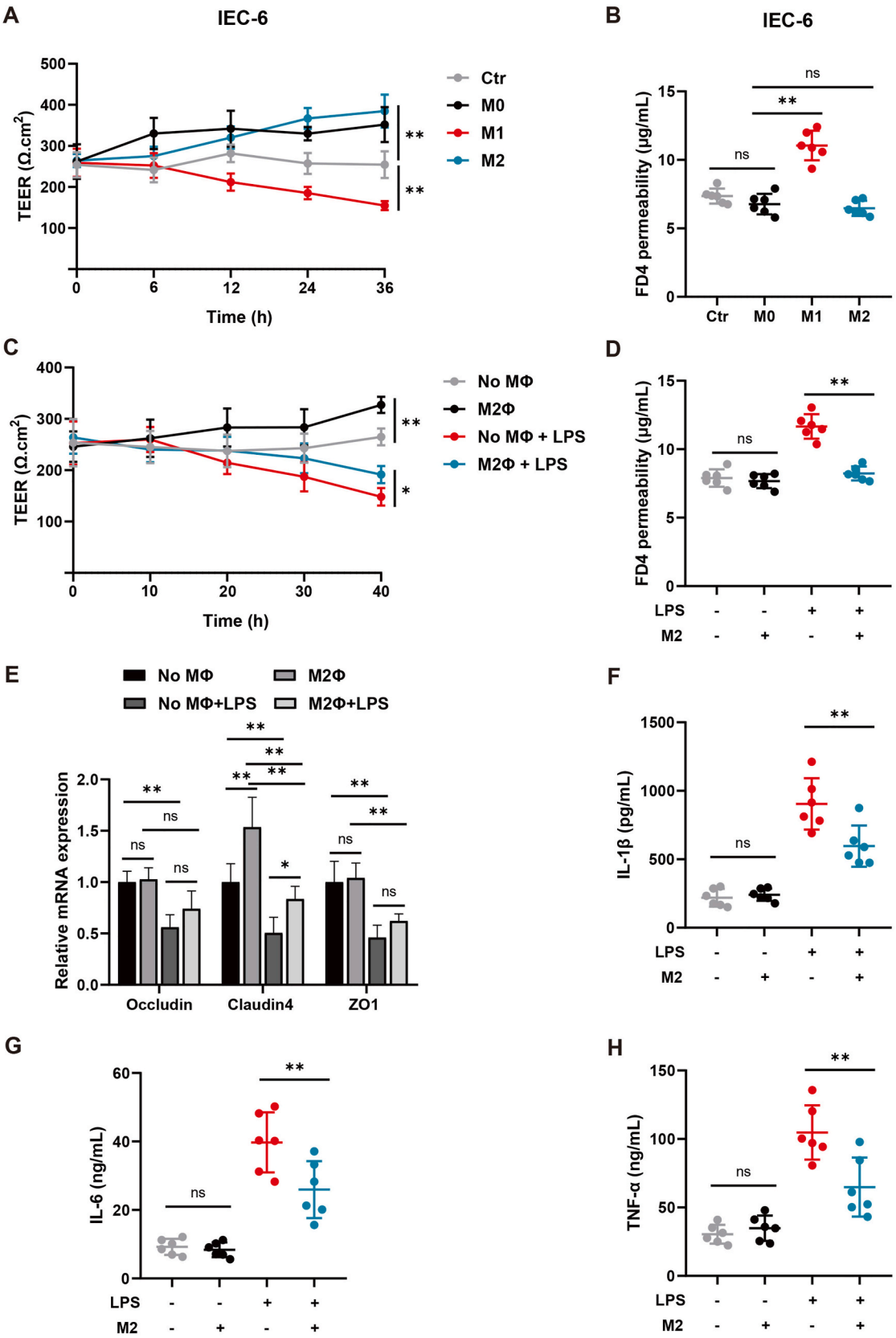

Fig. 1. Polarized M2-like macrophages contribute to alleviate intestinal inflammation. RAW264.7 cells were incubated with 100 ng/mL LPS plus 20 ng/mL IFN-γ or 50 ng/mL IL-4 for 48 h to induce polarization to the M1 or M2 phenotype. IEC-6 cells were then co-cultured with non-polarized (M0) or polarized macrophages (M1 or M2), respectively. (**A**) TEER of IEC-6 cells when co-cultured with differentially polarized macrophages for up to 36 h. (**B**) FD4 flux of IEC-6 cells when co-cultured with differentially polarized macrophages for 24 h. TEER (**C**), FD4 flux (**D**), mRNA expression of tight junction proteins (**E**), and the secretion of IL-1β (**F**), IL-6 (**G**), and TNF-α (**H**) in IEC-6 cells were also assayed with or without 12-h co-culture with M2 macrophages in the presence or absence of 10 μg/mL LPS. Data represent means ± SD of three separate experiments. Statistics was performed with one-way ANOVA, followed by Tukey's multiple comparison test. *$P < 0.05$, **$P < 0.01$.

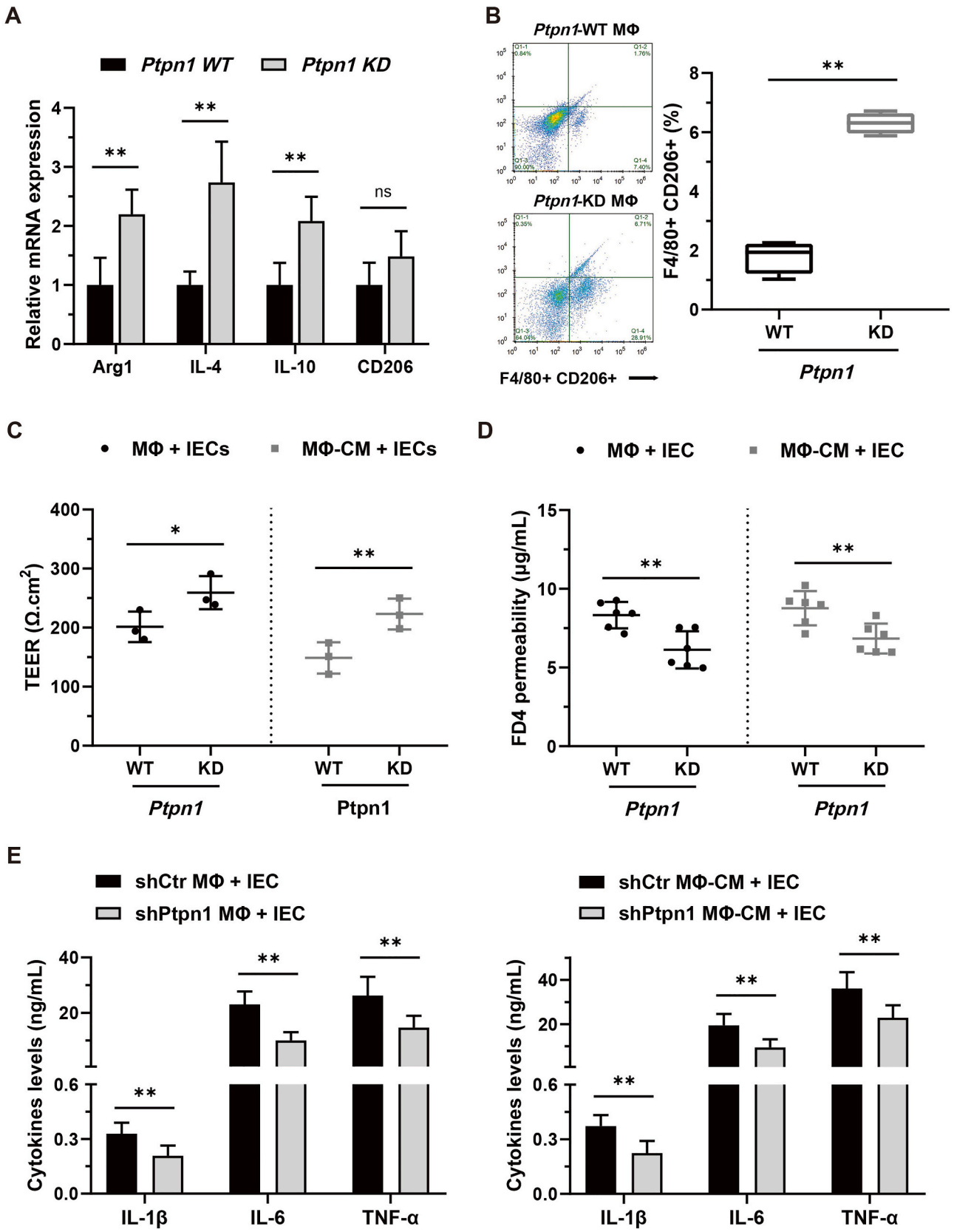

Fig. 2. *Ptpn1* knock-down (KD) promotes M2 macrophage polarization and intestinal barrier function, while reducing intestinal inflammation. RAW264.7 cells that were transfected with control shRNA or *Ptpn1* shRNA, followed by RT-qPCR analysis of *Arg1*, *Il4*, *Il10*, and *CD2*06 mRNA expression levels (**A**) or flow cytometry of the F4/80^{+}CD206^{+} population (**B**). IEC-6 cells were co-cultured with wild-type (WT) or *Ptpn1*-KD macrophages or conditioned medium collected from wild-type or *Ptpn1*-KD macrophages for 24 h, followed by measurement of TEER (**C**), FD4 flux (**D**), and proinflammatory cytokine levels (**E**). Data represent means ± SD of 8 animals/treatment. Statistics was performed with Student's *t*-test or one-way ANOVA, followed by Tukey's multiple comparison test. $^{*}P < 0.05$, $^{**}P < 0.01$.

2.10. Mouse experiments

Male C57BL/6 mice aged 8 weeks were purchased from SPF Biotechnology Co., Ltd (Beijing, China). The *Ptpn1*-knockout (KO) mice were generated in the Nanjing Biomedical Research Institute of Nanjing University (Nanjing, China). The transcript of Ptpn1-201 was selected for the generation of KO animals, which had a C57BL/6J background. All the offspring of ICR females (F0 mice) were identified by PCR and sequencing of tail DNA. Finally, crossing positive F0 mice with C57BL/6J mice were performed to produce heterozygous mice [17]. Male and female Ptpn1 heterozygous mice, maintained on mixed genetic C57BL/6J background, were intercrossed to yield three genotypes of mice. The global Ptpn1-deficient male mice aged 10 weeks were used in the experiments. Macrophages-derived sEVs (20 μg/mouse) or lactadherin were administered to mice every two days by intraperitoneal injection. After indicated time, mice were intraperitoneally injected with 10 mg/kg LPS in saline and then sampled 4 h later. To deplete macrophages, mice were administrated intraperitoneally with clodronate-loaded liposomes (200 μL/mouse) once every three days for three times. After macrophage depletion, 20 μg sEVs in 0.2 mL PBS were intraperitoneally injected into each mouse every two days for 10 days. For *Salmonella* Typhimurium infection, mice were inoculated with 1×10^7 CFU of *Salmonella* Typhimurium in 200 μL PBS by oral gavage and sampled three days later. All mouse procedures were approved by the China Agricultural University Animal Care and Use Committee (Approval No. AW52101202-2-1, Beijing, China).

2.11. Histology

For histological analysis, the colon of mice was harvested. Hematoxylin/eosin (H&E) and immunohistochemical staining were performed according to standard protocols. The histology score was determined as previously described [25].

2.12. Flow cytometry

A segment of the jejunum and colon tissues were minced and digested, and the resulting cell suspension was centrifuged at 12 000×g for 5 min. The cells were harvested and then incubated with antibodies specific to F4/80, CD11b, CD11c, or CD206 for 30 min. Cells were then washed three times and subjected to flow cytometry on BD FACSAria II Cell Sorter (BD Biosciences, New Jersey, USA). For efferocytic capacity analysis, macrophages were incubated with apoptotic cells labelled with the fluorescent dye PKH67 dye for 45 min followed by apoptotic cell removal. After 2 h of further incubation, the macrophages were detached and sorted by flow cytometry to isolate apoptotic cell-positive and apoptotic cell-negative macrophages.

2.13. Lactadherin neutralization

For the neutralization experiments, indicated mice were intraperitoneally injected with anti-lactadherin-specific mAb (R&D Systems, AF2805) once every two days for twice at a dose of 100 μg per mouse. The control groups received isotype control IgG2α mAb.

2.14. Ussing chamber

Ussing chamber experiments were performed as previously described [10]. In brief, the mucosa tissue was mounted on Ussing chamber inserts and 5 mL of oxygenated Ringers' solution (Solarbio, Beijing, China) added bilaterally. The tissue was allowed to equilibrate for 20 min, followed by an addition of FD4 (80 mg mL^{-1}) and 70 kDa Rhodamine-Dextran (RD70; 20 mg mL^{-1}) to the apical side. After 2 h, 100 μL Ringers' solution was removed from the serosal side for measurement of FD4 and RD70.

2.15. Luciferase assay

IEC-6 cells were stably transfected with an NF-κB luciferase reporter vector (SL-0012, Signosis, Santa Clara, CA, USA) and grown according to the manufacturers' instructions, and luciferase activity was measured (Promega, Madison, WI, USA).

2.16. Statistical analyses

Statistics was performed using Student's *t*-test for two group and one-way analysis of variance (ANOVA) followed by Tukey's *post hoc* test using SPSS 21.0 (SPSS Inc., Chicago, IL, USA). For all analyses, $P < 0.05$ was considered significant.

3. Results

3.1. Polarity of macrophages differentially regulates intestinal epithelial barrier function and inflammation

To understand how differentially polarized macrophages affect intestinal epithelial barrier integrity, IEC-6 cells were co-cultured with non-polarized (M0), M1-or M2-polarized RAW264.7 macrophages for 24 h. As expected, co-culture with M1 macrophages significantly decreased the TEER of IEC-6 cells (Fig. 1A) and increased 4-kDa FITC-dextran (FD4) permeability (Fig. 1B), consistent with reduced intestinal barrier integrity. On the other hand, M0 or M2 macrophages significantly enhanced TEER of IEC-6 cells (Fig. 1A) with a tendency to reduce FD4 permeability (Fig. 1B) and increased Claudin-4 mRNA expression (Supplementary Fig. 1A), suggestive of enhanced barrier function. Co-culture with M2 macrophages also reduced LDH release, redox-active iron overload, and intracellular ROS generation in MODE-K or IEC-6 cells, while M1 macrophages had an opposite effect (Supplementary Figs. 1B–D). A similar effect was observed in IECs cultured in RAW264.7 conditioned medium (Supplementary Figs. 1E and F). To further investigate whether polarized macrophages differentially regulate intestinal inflammation, M2 macrophages were co-cultured with LPS-stimulated IEC-6 cells. As expected, LPS significantly reduced TEER (Fig. 1C) and tight junction protein gene expression (Fig. 1E), while increasing FD4 flux (Fig. 1d) and inflammatory cytokine levels including IL-1β, IL-6 and TNF-α (Fig. 1F–H) in IEC-6 cells. However, co-culture with M2 macrophages significantly reversed the detrimental effect in LPS-treated IEC-6 cells (Fig. 1C–H). Collectively, these results indicated that alternatively activated, M2-like macrophages are capable of alleviating epithelial inflammation and promoting intestinal barrier function.

3.2. Ptpn1 knockdown promotes M2 macrophage polarization and restores intestinal homeostasis

Ptpn1 is known to regulate macrophage polarization [16,17]. To assess the role of Ptpn1 in epithelial function, *Ptpn1* was knocked down in RAW264.7 cells using shRNA-mediated RNA interference. The knockdown (KD) efficiency was confirmed to be approximately 70% (Supplementary Fig. 2A). The expression levels of M2 marker genes including *Arg1*, *Il4*, *Il10,* and *CD206* were significantly increased in *Ptpn1*-KD macrophages (Fig. 2a). Consistently, we observed an increase in the frequency of $F4/80^{+}CD206^{+}$ M2-like phenotype in RAW264.7 cells following *Ptpn1*-KD (Fig. 2B). To investigate whether PTPN1 knockdown could affect IEC-macrophage interactions and epithelial function, IEC-6 cells were co-cultured with *Ptpn1* knockdown macrophages and found to show an increased TEER (Fig. 2C) and reduced FD4 permeability (Fig. 2D) and inflammatory cytokine expressions (Fig. 2E). The mRNA expression levels of *claudin 4* and *ZO1*, but not *occludin*, were significantly increased in IEC-6 cells when co-cultured with *Ptpn1*-KD macrophages (Supplementary Fig. 2B), while the viability of RAW264.7 or IEC-6 was unaffected by the treatment (Supplemental Figs. 2C and D).

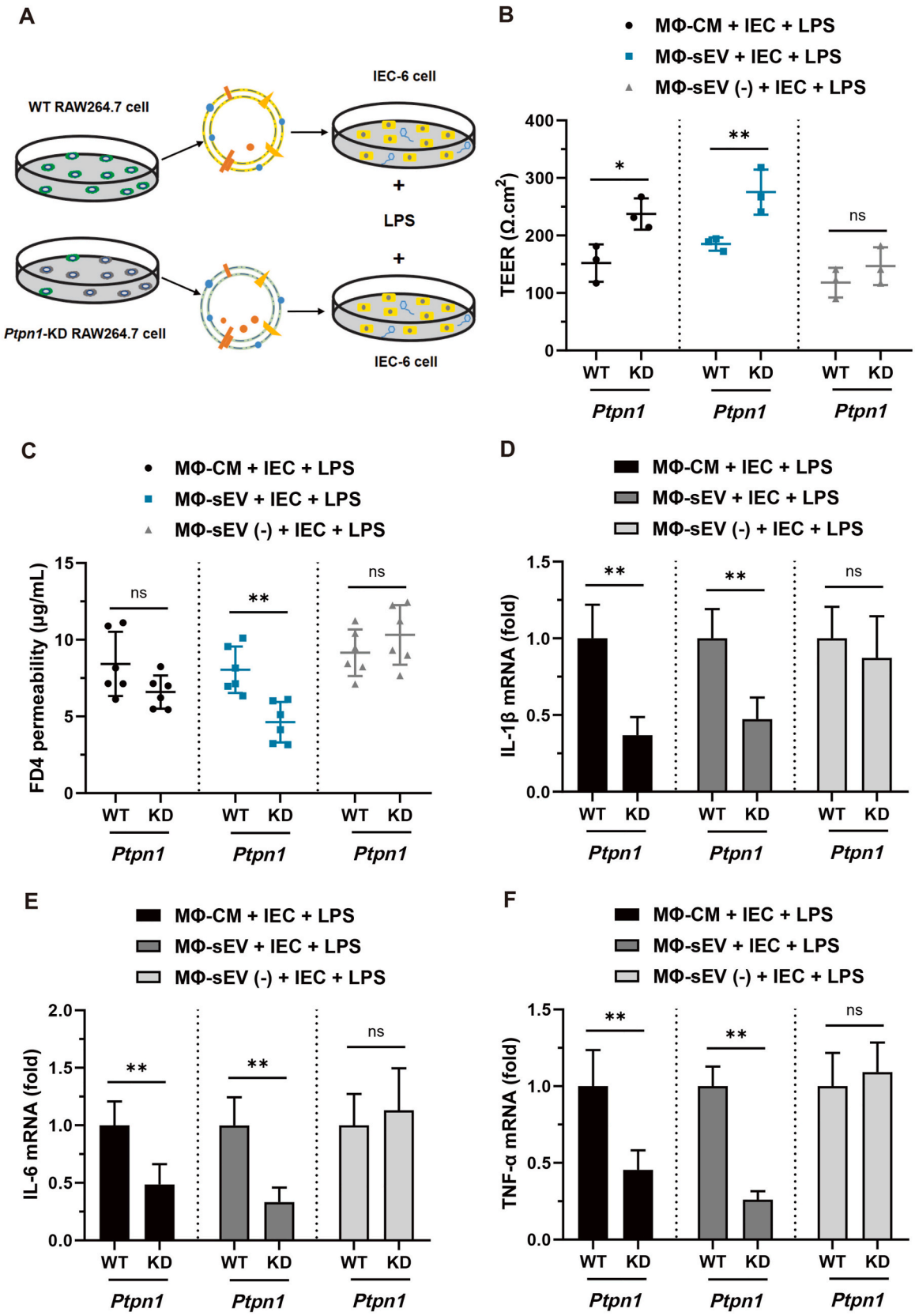

Fig. 3. Small extracellular vesicles mediate the communication between macrophages and IEC-6 cells. (**A**) Schematic diagram of the experimental design. IEC-6 cells were stimulated with LPS (10 μg/mL) for 12 h or 24 h, followed by incubation with conditioned medium, sEVs, and sEVs-depleted conditioned medium from either WT or *Ptpn1*-KD RAW264.7 macrophages for another 12 h. TEER (**B**), FD4 flux (**C**), and mRNA levels of *Il1β* (**D**), *Il6* (**E**), and *Tnfα* (**F**) were measured in IEC-6 cells. Data represent means ± SD of three separate experiments. Statistics was performed with Student's *t*-test or one-way ANOVA, followed by Tukey's multiple comparison test. $*P < 0.05$, $**P < 0.01$.

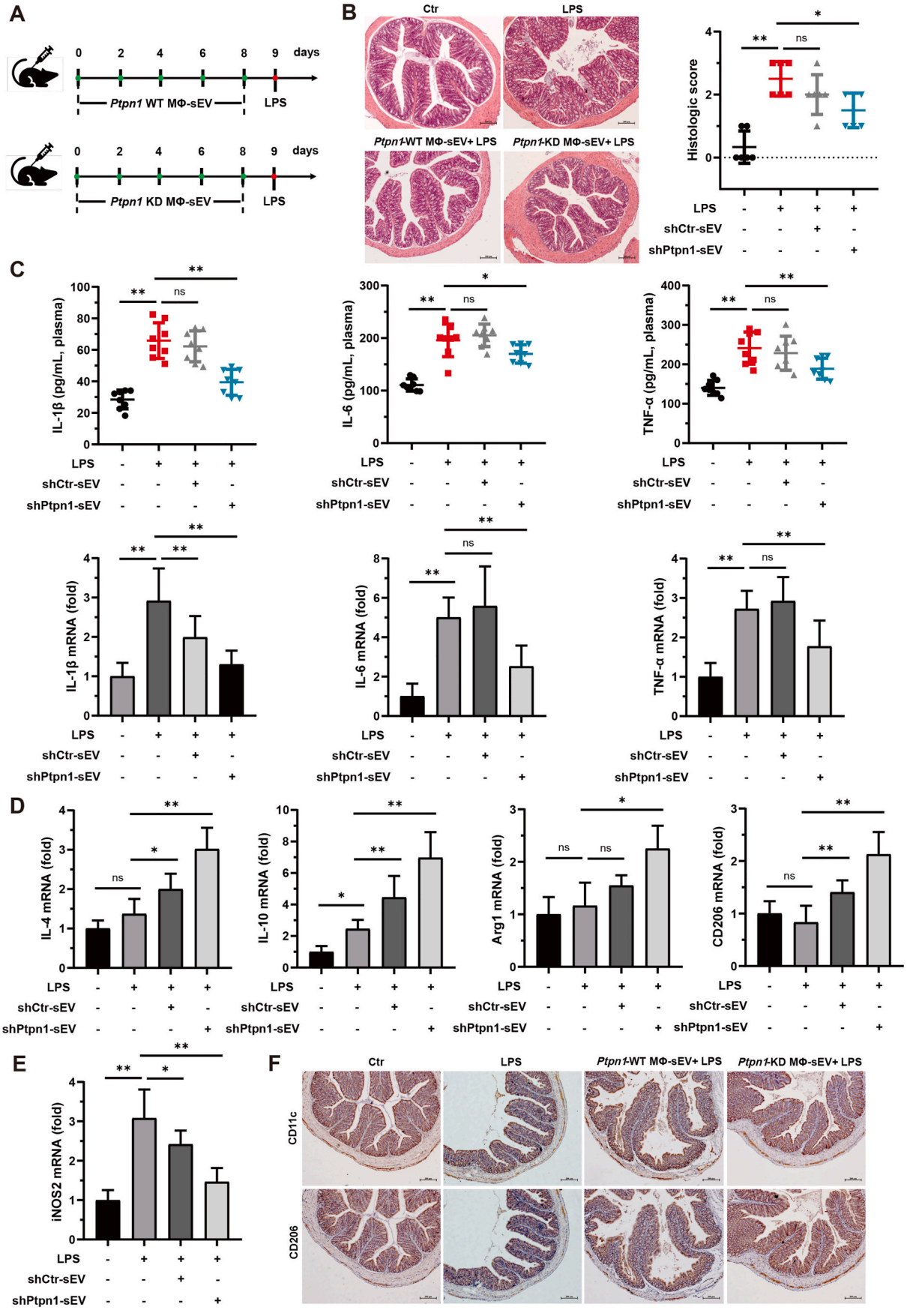

(caption on next page)

Fig. 4. Small extracellular vesicles derived from *Ptpn1*-KD macrophages induce M2 polarization of intestinal macrophages and suppress inflammatory response in mice. (**A**) Schematic diagram of the experimental design. Mice (n = 8) were intraperitoneally injected with sEVs (20 μg/mouse) isolated from either WT or *Ptpn1*-KD RAW 264.7 macrophages once every 2 days for five times, followed by intraperitoneal administration of 10 mg/kg LPS on day 9. Animals were sacrificed for sample collection and analysis 4 h later. (**B**) H&E staining (scale bar = 200 μm) and histology score of the colon. (**C**) Expressions of inflammatory cytokines including TNF-α, IL-1β, and IL-6 in the serum (top panels) and the colon (bottom panels). (**D**) mRNA expression levels of M2 macrophage marker genes in the colon. (**E**) mRNA expression of *iNOS 2*, a M1 marker gene in the colon. (**F**) Prevalence of $CD206^+$ macrophages and $CD11b^+$ macrophages in the colon as revealed by IHC staining. Data represent means ± SD of 8 animals/treatment. Statistics was performed with one-way ANOVA, followed by Tukey's multiple comparison test. $^*P < 0.05$, $^{**}P < 0.01$.

Importantly, we observed that the conditioned medium from *Ptpn1* knockdown macrophages achieved much of the same barrier-enhancing and anti-inflammatory effects as *Ptpn1* knockdown macrophages *per se* (Fig. 2C–E). Together, these results suggested that Ptpn1 is responsible for promoting M1 macrophage polarization and intestinal inflammation.

3.3. Small extracellular vesicles confer the barrier-enhancing and anti-inflammatory effect of Ptpn1 knockdown macrophages in the macrophage-IEC co-culture system

Macrophages and IECs interact with each other by exchanging soluble effectors such as exomes, which are known to be critical in intercellular communication [21,23,25,26]. To directly examine the role of sEVs in mediating the anti-inflammatory effect of *Ptpn1*-KD macrophages on IECs, we purified exomes from conditioned media of both *Ptpn1*-WT and *Ptpn1*-KD macrophages, labelled them with a red fluorescent dye, DiI, and applied them in a co-culture system with IEC-6 cells. Small extracellular vesicles derived from macrophages exhibited typical intact cup-shaped membrane vesicles with an average size of 110 nm by transmission electron microscopy (TEM; Supplementary Fig. 3B). In addition, nanoparticle tracking analysis (NTA) revealed that these sEVs had diameters ranging from 10 to 500 nm, with a mean diameter of 120 nm (Supplementary Fig. 3C). To further characterize the sEVs in our preparations, sEVs -specific markers, CD63 and Alix, were confirmed to be expressed on the sEVs of both *Ptpn1*-WT and *Ptpn1*-KD macrophages by Western blotting. The calnexin expression in isolated fractions was also detected by Western blotting to demonstrate absence of endoplasmic reticulum (Supplementary Fig. 3D) To our surprise, IEC-6 and macrophages were much more efficient in taking up *Ptpn1*-KD sEVs than *Ptpn1*-WT sEVs (Supplementary Fig. 3E), implying that *Ptpn1* knockdown is beneficial for cellular uptake of sEVs.

To further explore whether sEVs directly mediate the macrophage-IEC crosstalk, IEC-6 cells were first stimulated with LPS for 24 h and then cultured with conditioned medium, sEVs, or sEVs-depleted conditioned medium from either *Ptpn1*-WT or *Ptpn1*-KD RAW264.7 macrophages (Fig. 3A). As expected, *Ptpn1*-KD macrophage-conditioned medium significantly increased TEER (Fig. 3B), but decreased FD4 permeability (Fig. 3c) and pro-inflammatory cytokines IL-1β, IL-6 and TNF-α (Fig. 3D–F) in LPS-stimulated IEC-6 cells. While the levels of anti-inflammatory cytokine IL-10 was unaffected in the conditioned medium, sEVs, or sEVs-depleted conditioned medium from either Ptpn1-WT or Ptpn1-KD RAW264.7 macrophages (Supplemental Fig. 4A). A similar result was observed with IEC-6 cells exposed to sEVs derived from *Ptpn1*-KD macrophages (Fig. 3), while neither macrophage-conditioned medium nor macrophage-sEVs have any effect on cell viability (Supplementary Fig. 2D, and Supplementary Fig. 4B). Notably, sEVs-depleted medium lost much of the beneficial effect of *Ptpn1*-KD macrophages on barrier function and inflammation (Fig. 3). Collectively, these results strongly suggested that sEVs secreted from macrophages play a major role in mediating the macrophage-IEC crosstalk.

3.4. Ptpn1 knockdown macrophage sEVs enhance M2 polarization and mitigate intestinal inflammation in vivo

To further examine whether sEVs derived from *Ptpn1*-KD macrophages could induce M2 macrophage polarization and suppress inflammation *in vivo*, mice were administered with or without sEVs isolated from *Ptpn1*-WT or *Ptpn1*-KD macrophages, followed by a 4-h LPS challenge (Fig. 4A). In line with our in vitro co-culture results, sEVs from *Ptpn1*-KD, but not *Ptpn1*-WT, macrophages significantly alleviated LPS-induced intestinal pathology and histology score, as evidenced by exfoliation of epithelial cells, hyperaemia, inflammatory exudation, epithelial cell shedding, mucosal disintegration, and shedding of microvilli in the colon (Fig. 4B). Similarly, markers of systemic and colonic inflammation, including *Tnfα*, *Il1β*, and *Il6* inflammatory cytokines, were also strikingly reduced in response to LPS when administered with *Ptpn1*-KD, but not *Ptpn1*-WT, macrophage sEVs (Fig. 4C).

To confirm whether sEVs-mediated reduction of intestinal inflammation was achieved through modulating macrophage polarization, we examined the expressions of M1 and M2 macrophage marker genes in the colon of mice. Relative to the *Ptpn1*-WT macrophage sEVs, administration of *Ptpn1*-KD macrophage sEVs induced the expressions of all four M2 marker genes examined (*Arg1*, *CD206*, *Il4*, and *Il10*) (Fig. 4D), but suppressed *iNOS 1*, an M1 maker gene, in the colon (Fig. 4E). Immunohistochemistry further revealed that administration of *Ptpn1*-KD macrophage sEVs obviously increased the prevalence of $CD206^+$, M2-like macrophages, but reduced the populations of $CD11c^+$, M1-like macrophages in the colon (Fig. 4F, and Supplementary Fig. 5A). Moreover, flow cytometry confirmed a significant increase in the frequency of $F4/80^+CD206^+$, M2 macrophages (Supplementary Fig. 5B) with a concomitant decrease of $CD11b^+CD11c^+$, M1 macrophages in the colon (Supplementary Fig. 5C) in response to administration of *Ptpn1*-KD macrophage sEVs. These results collectively suggested that *Ptpn1* KD favors M2 polarization and reduces intestinal inflammation and that sEVs are mainly responsible for conferring the beneficial effect.

3.5. Ptpn1 knockdown macrophage sEVs protect mice from intestinal infection in a macrophage-dependent manner

To further confirm whether macrophages are required for sEVs-mediated resolution of intestinal inflammation, a model of *Salmonella* Typhimurium infection was employed using macrophage-depleted mice. Mice were injected with clodronate-loaded liposomes to deplete macrophages, followed by intraperitoneal administration of *Ptpn1*-KD macrophage sEVs for 10 days and a challenge with *Salmonella* Typhimurium for another three days (Fig. 5A). As expected, mice exhibited obvious intestinal inflammation and colon shortening if left untreated; however, the symptoms were notably alleviated by sEVs administration, as evidenced by reduced weight loss (Fig. 5B) and infiltration of inflammatory cells in the colonic mucosa (Fig. 5C), and a relief of colon shortening (Fig. 5D). Moreover, sEVs administration obviously inhibited the release of inflammatory cytokines IL-1β, IL-6 and TNF-α (Fig. 5E), consistent with reduced intestinal mucosal inflammation. Importantly, sEVs failed to ameliorate intestinal inflammation in macrophage-depleted mice (Fig. 5B–E), suggesting a requirement of macrophages in sEVs-mediated protection.

3.6. Ptpn1 deficiency alters macrophage sEVs protein contents with the enrichment of lactadherin

To examine whether proteins are differentially present in the sEVs of WT and *Ptpn1*-KD RAW264.7 cells, triple-quadrupole mass spectrometry was conducted. A number of proteins were differentially enriched in *Ptpn1*-KD RAW264.7 cells (Supplementary Table S1). Among them is lactadherin, also known as milk fat globule-EGF factor 8 protein (MFG-

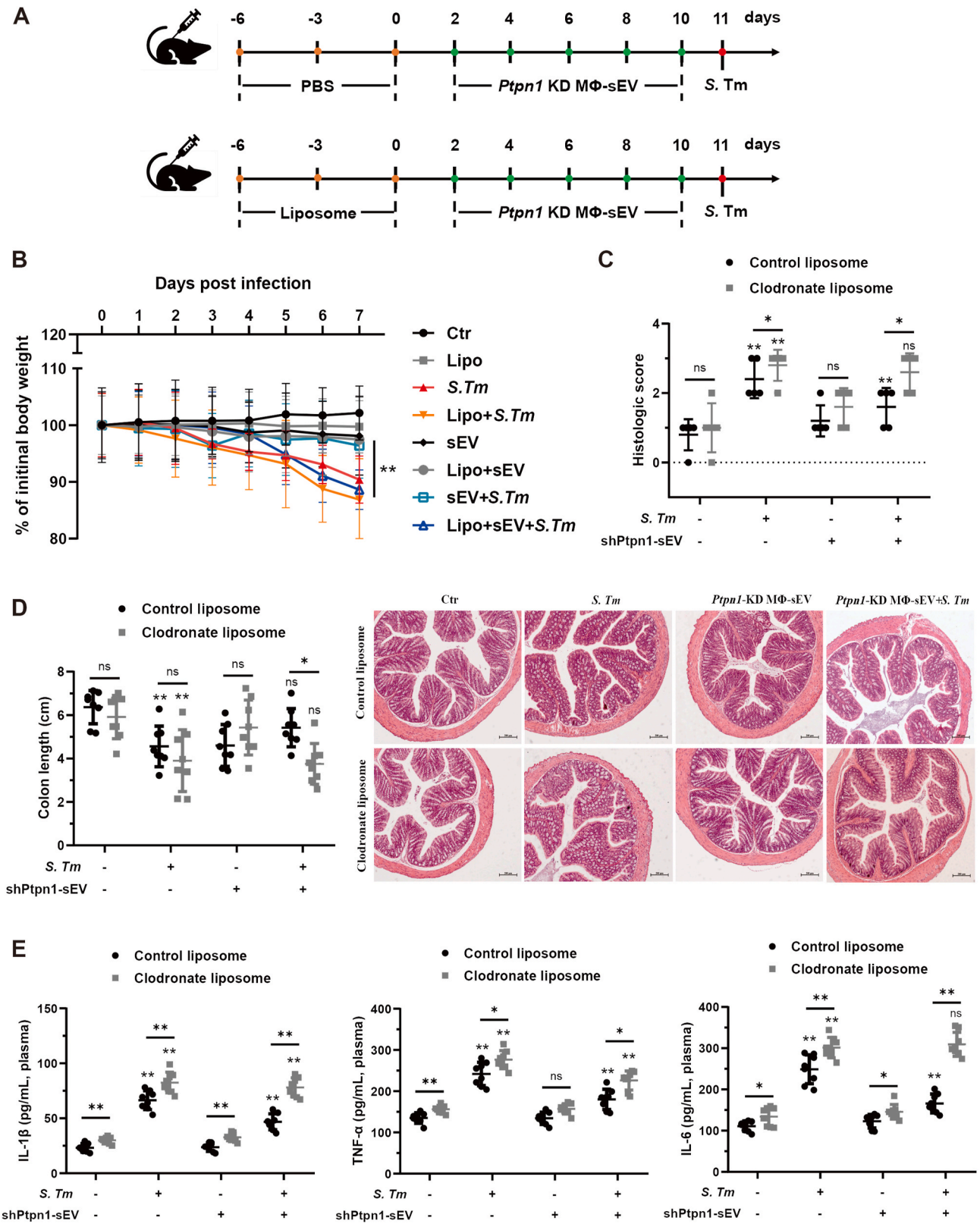

Fig. 5. Macrophage depletion diminishes the protective effect of *Ptpn1*-KD macrophage small extracellular vesicles against *Salmonella* Typhimurium infection. (**A**) Schematic diagram of the experimental design. Macrophages were depleted in mice by intraperitoneal administration of clodronate-loaded liposomes every three days for three times, followed by intraperitoneal injection of PBS or *Ptpn1*-KD sEVs for another five times. Mice (n = 8) were then infected with *Salmonella* Typhimurium and sampled three days later. Disease severity was measured as indicated by body weight loss (**B**), histology (**C**), and colon length (**D**). (**E**) Serum levels of inflammatory cytokines including TNF-α, IL-1β, and IL-6. Data represent means ± SD of 8 animals/treatment. Statistics was performed with Student's *t*-test or one-way ANOVA, followed by Tukey's multiple comparison test. $^{*}P < 0.05$, $^{**}P < 0.01$.

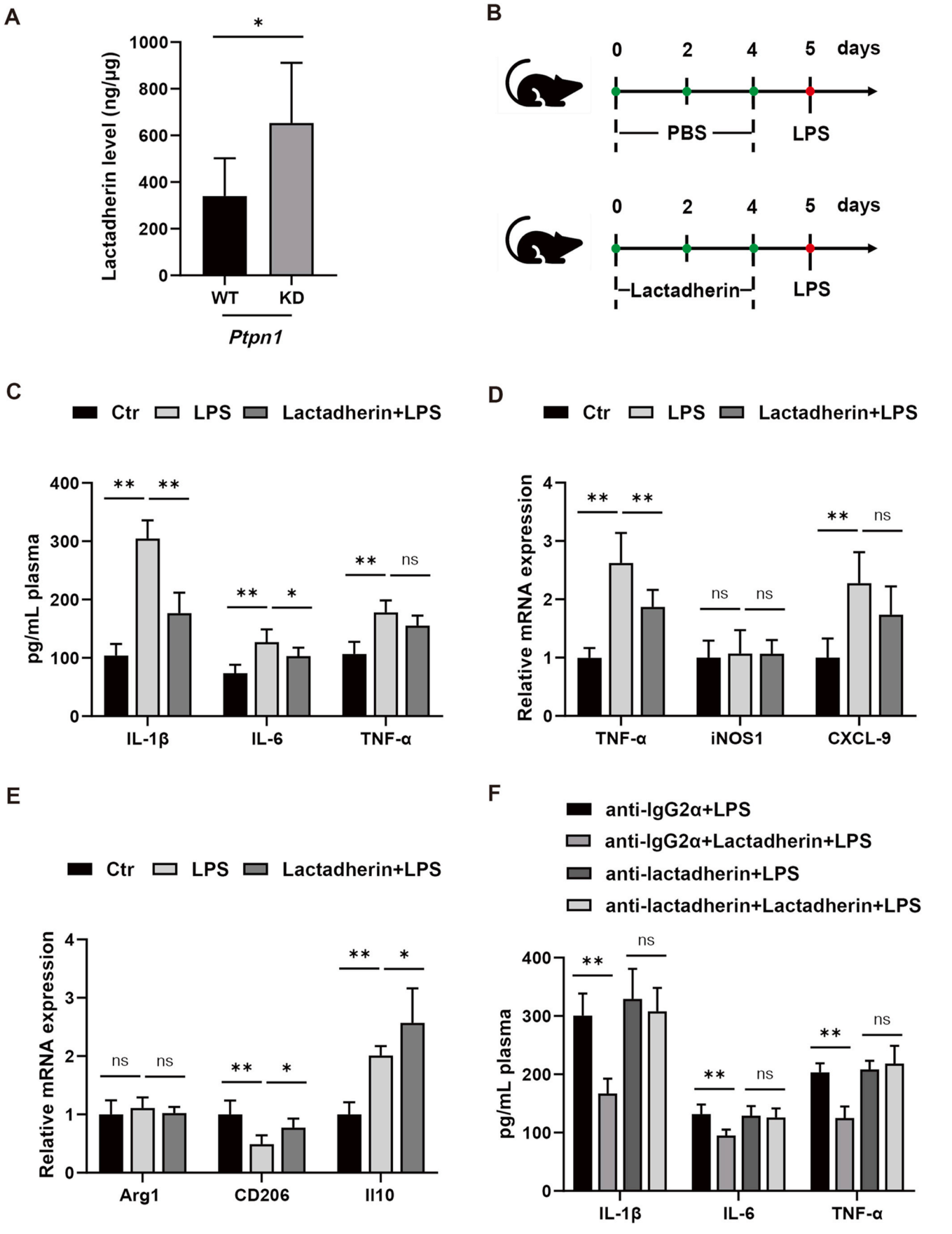

(caption on next page)

Fig. 6. Lactadherin enriched in *Ptpn1*-KD macrophage small extracellular vesicles ameliorates intestinal inflammation. (A) Lactadherin levels in the exomes of WT and *Ptpn1*-KD macrophages. (**B**) Schematic diagram of the experimental design. Mice were intraperitoneally injected with lactadherin (20 μg/mouse) or an equal volume of PBS once every 2 days for three times, followed by intraperitoneal administration of 10 mg/kg LPS on day 5. Animals were sacrificed for sample collection and analysis 4 h later. (**C**) Serum levels of inflammatory cytokines including TNF-α, IL-1β, and IL-6. (**D**) mRNA expression levels of M1-characteristic *Tnfa*, *iNOS* and *Cxcl9*, and (**E**) M2-characteristic *Arg1*, *CD206* and *Il10* in the colon. *Ptpn1* KO mice were intraperitoneally injected with anti-lactadherin-specific mAb (100 μg per mouse) an indicated time and then administrated with lactadherin (20 μg/mouse) or an equal volume of PBS once every 2 days for three times, followed by intraperitoneal injection of 10 mg/kg LPS on day 5. Animals were sacrificed for sample collection and analysis 4 h later. (**F**) Serum levels of inflammatory cytokines including TNF-α, IL-1β, and IL-6. Data represent means ± SD of 8 animals/treatment. Statistics was performed with Student's *t*-test or one-way ANOVA, followed by Tukey's multiple comparison test. $^{*}P < 0.05$, $^{**}P < 0.01$.

E8), with a well-documented role in modulating macrophage polarization and intestinal inflammation [27,28]. Lactadherin was measured to be 340.48 and 654.14 ng/μg sEVs proteins of WT and *Ptpn1*-KD RAW264.7 cells, respectively (Fig. 6A).

3.7. Recombinant lactadherin alleviates intestinal inflammation by inducing M2 macrophage polarization

To examine whether lactadherin is capable of suppressing intestinal inflammation, mice were intraperitoneally administered with recombinant lactadherin, followed by a 4-h LPS challenge (Fig. 6B). Lactadherin was effective in suppressing intestinal inflammatory cytokine expression (Fig. 6C), but there was no effect on gut barrier function besides the increased TEER *ex vivo* (Supplementary Fig. 6). Given that the beneficial effect of *Ptpn1*-KD macrophage sEVs was achieved through enhancing M2 macrophage polarization, we next examined the expressions of M1 and M2 macrophage marker genes in the colon of lactadherin-treated mice. As expected, LPS significantly elevated the expressions of M1 marker genes such as *Tnfa* and *Cxcl9* (Fig. 6D), but they were suppressed in response to administration with lactadherin. On the other hand, lactadherin obviously increased the mRNA expression of M2 marker genes such as *CD206* and *Il10* (Fig. 6E). *In vitro* studies with RAW264.7 cells further confirmed the ability of lactadherin to induce M2 polarization (Supplementary Fig. 7A). These results suggested that lactadherin mitigates intestinal inflammation by shifting macrophages from the M1 to M2 phenotype. To further confirmed the functional role of sEVs lactadherin on *Ptpn1*-mediated intestinal inflammation, we also used neutralizing anti-lactadherin in *Ptpn1* KO mice. As expected, the increased inflammatory cytokines induced by LPS treatment were not affected after lactadherin neutralization in *Ptpn1* KO mice (Fig. 6F). These data provided definitive evidences on the contribution of the functional role of sEVs lactadherin in inhibiting Ptpn1-mediated intestinal inflammation. Given the key role of lactadherin in the acceleration of efferocytosis and improving the clearance of dying cells, we reasoned that lactadherin might be involved in Ptpn1-mediated enhancement of efferocytosis by macrophages during inflammation resolution. Accordingly, we asked another question that whether lactadherin would enhance efferocytic capacity of the macrophage. We found that lactadherin significantly increased the number of apoptotic cell-positive macrophages (Supplementary Fig. 7B). This suggested that the anti-inflammatory effect of lactadherin was achieved through promoting the efferocytic capacity of macrophage and the clearance of apoptotic cells.

3.8. Lactadherin exerts anti-inflammatory effect by suppressing TNF-α and NF-κB signalling

To further explore whether lactadherin could directly influence intestinal barrier function, IECs were first treated with lactadherin for 24 h and then stimulated with LPS. Similarly, lactadherin significantly increased TEER (Fig. 7A) and *occudin* mRNA expression (Supplementary Fig. 8A) in both IEC-6 and IPEC-1 cells. However, *ZO1*, *claudin-1*, *Muc 1* and *Muc 2* mRNA levels appeared to be unaffected by lactadherin (Supplementary Fig. 8A). Lactadherin also significantly suppressed LPS-induced inflammatory cytokine expressions in IEC-6 and IPEC-1 cells (Fig. 7B). Additionally, lactadherin markedly enhanced survival and reduced apoptosis of IECs challenged with LPS (Supplementary Fig. 8C). These results implied that lactadherin improves intestinal barrier function by suppressing inflammation. Activation of NF-κB is well-known to exacerbate intestinal inflammation and M1 macrophage polarization. To better understand the mechanism of lactadherin-mediated antiinflammatory and barrier-protective activities, we next sought to investigate that the direct impact of lactadherin on the NF-κB signalling pathway. We found that lactadherin significantly decreased LPS-induced *Tlr4* mRNA level (Fig. 7C) and NF-κB reporter activity in IEC-6 cells (Fig. 7D).

4. Discussion

The central goal of this study was to investigate the impact of Ptpn1 and macrophage-derived sEVs on macrophage-IEC interactions in the context of intestinal inflammation. Toward this, we co-cultured *Ptpn1*-KD macrophages with LPS-stimulated IECs to identify how Ptpn1 influence the crosstalk between macrophage and IECs. Macrophage-deleted mice were administered with the sEVs from *Ptpn1*-deficient macrophages in LPS or *Salmonella* Typhimurium model of intestinal inflammation. We have shown that Ptpn1 is critically important in regulating the macrophage-IEC crosstalk and that Ptpn1 deficiency drives M2 macrophage polarization, which in turn promotes intestinal barrier integrity and inflammation resolution. Impressively, sEVs released from *Ptpn1*-KD macrophages is capable of alleviating intestinal inflammation via delivery of the cargo containing lactadherin, leading to macrophage reprogramming and NF-κB inhibition (Fig. 8). Our findings suggest that lactadherin-enriched sEVs from *Ptpn1*-KD macrophage constitute an effective therapeutic approach to reducing intestinal inflammation.

It is well accepted that the heterogeneity of macrophages is influenced by intestinal microenvironment, which provides a variety of signals that direct the polarization of macrophages towards to distinct phenotypes [10,29–31]. A causal link between macrophage polarization and intestinal homeostasis has been established [10,32]. Classically activated M1 macrophages disrupt epithelial homeostasis by enhancing cytokine synthesis and barrier dysfunction in epithelial cells, ultimately causing bacterial translocation [31,32]. On the other hand, alternatively activated M2 macrophages promote the expression of barrier-sealing tight junction proteins and secret anti-inflammatory cytokines such as IL-10 to promote intestinal barrier integrity [9–11]. Notably, *Ptpn1*-deficient macrophages are M2-like with an intrinsic capability to produce higher levels of anti-inflammatory Il10 and tight junction proteins, contributing to inflammation resolution of IECs.

Ptpn1 is involved in inflammation by reprogramming macrophage polarization [14,16,33]. Mice that are globally deficient for Ptpn1 show enhanced barrier integrity in non-alcoholic steatohepatitis (NASH) [14]. However, recent studies have demonstrated a dual role of Ptpn1 in the progression and reversion of NASH [15]. Ptpn1 deficiency restricts the activation process of macrophages that is accompanied by the development of systemic inflammation [12,16]. Despite a dual role of Ptpn1 in non-immune and immune cells [34–37], much less is known on the involvement of Ptpn1 during intestinal inflammation progression. Polarized macrophages exhibit higher levels of *Ptpn1* mRNA than non-polarized macrophages, indicating that Ptpn1 activates macrophage polarization and function in response to different stressors such as

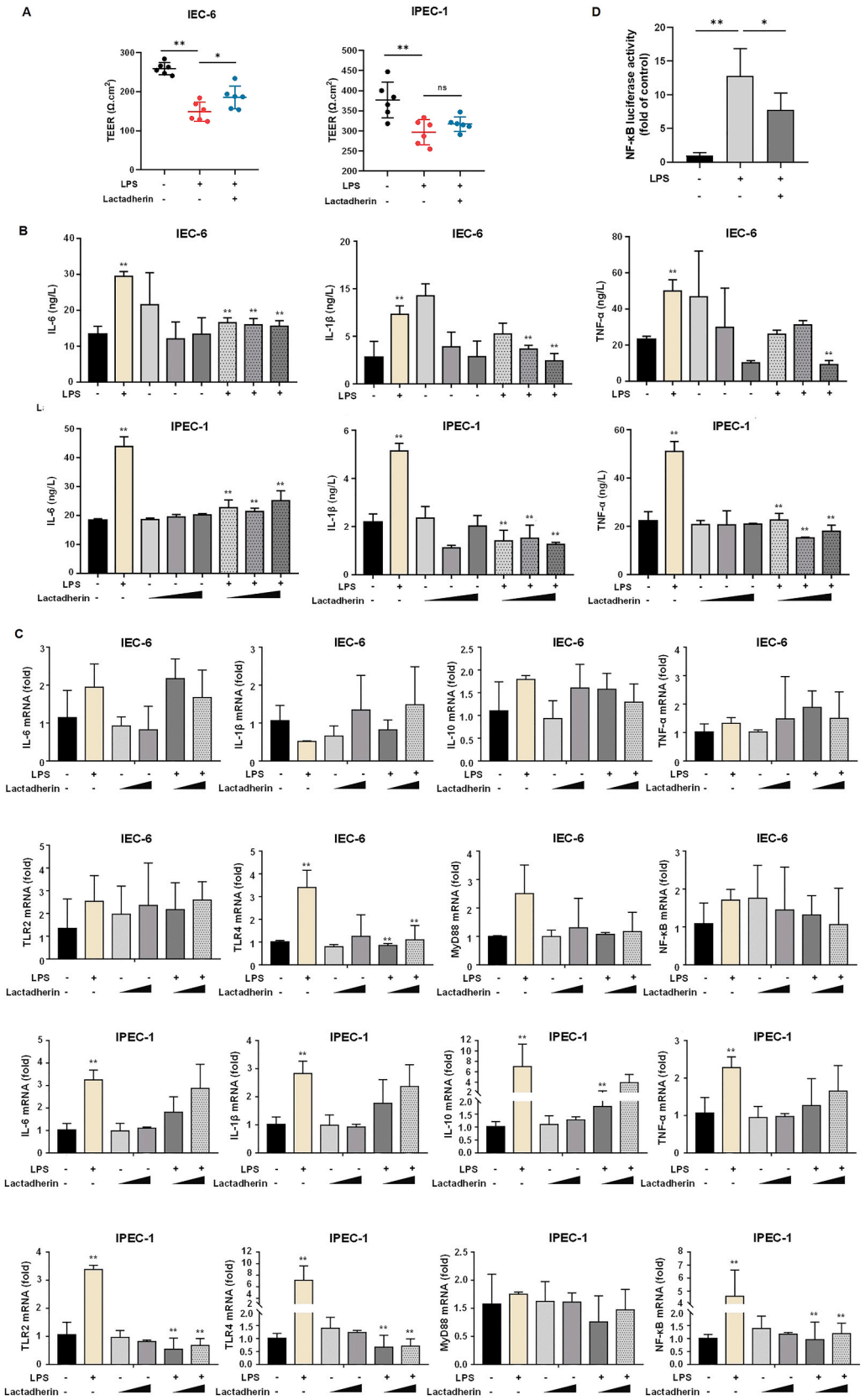

Fig. 7. The anti-inflammatory effect of lactadherin is achieved through inhibition of Nfκb. Intestinal epithelial cells (IEC-6 and IPEC-1) were incubated with or without lactadherin (25, 50, and 100 ng/mL) for 24 h, followed by stimulation with 10 μg/mL LPS for another 24 h. TEER (**A**) and the secretion of TNF-α, IL-1β, and IL-6 (**B**) as well as the mRNA expressions of *Il6*, *Il1β*, *Il10*, *Tnfa*, *Tlr2, Tlr-4, MyD88* and *Nfκb* (**C**) were measured in IEC-6 and IPEC-1 cells. (**D**) Lactadherin suppressed NF-κB activation in NF-κB -luciferase reporter cells. Data represent means ± SD of three separate experiments. Statistics was performed with one-way ANOVA, followed by Tukey's multiple comparison test. $^{*}P < 0.05$, $^{**}P < 0.01$.

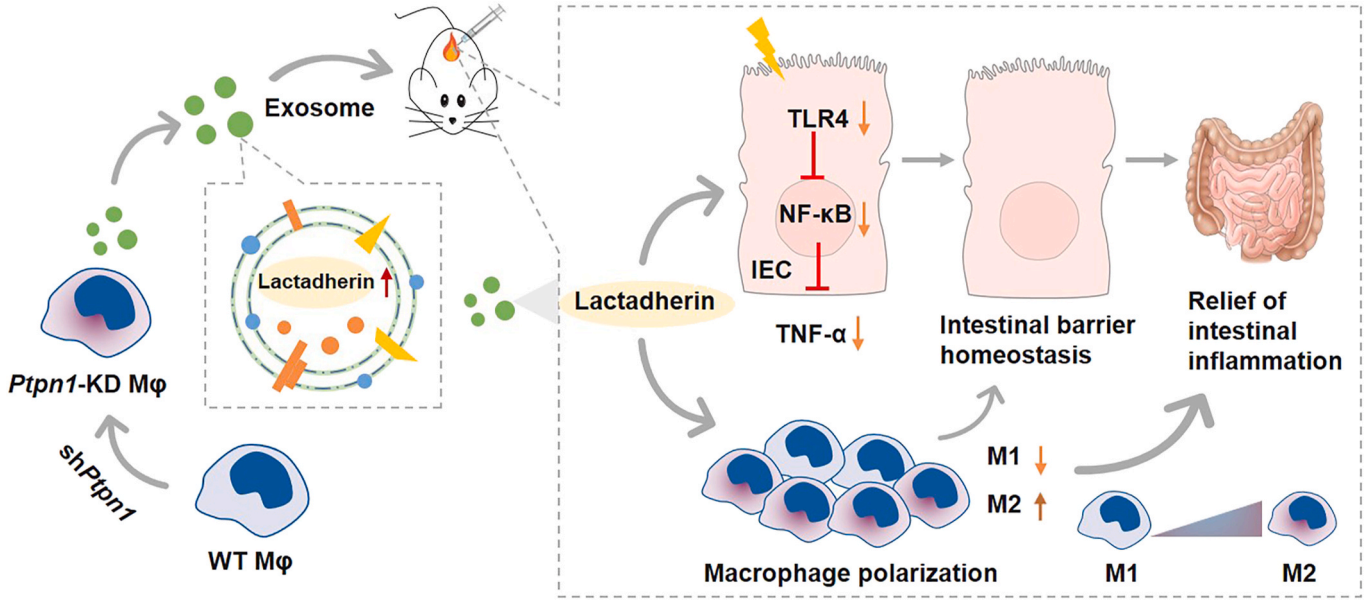

Fig. 8. Schematic illustration of small extracellular vesicle -mediated macrophage reprogramming. Small extracellular vesicles isolated from *Ptpn1*-KD macrophages induces M2 macrophage polarization and alleviates intestinal inflammation through enrichment of lactadherin, which subsequently inhibits NF-κB activation and causes M2 polarization of macrophages.

LPS challenge or IL-4 exposure. In this study, we investigated whether Ptpn1 deficiency in macrophages affects the response of IECs mediated by macrophage polarization. Ptpn1 knockdown enhances the communication between IECs and macrophages, as evidenced by promoting barrier integrity and decreasing inflammatory factors. Additionally, Ptpn1 deficiency also shifts macrophages towards to the anti-inflammatory M2 phenotype, suggesting a pro-inflammatory role for Ptpn1.

Although Ptpn1 plays a pivotal role in both pro-inflammatory and anti-inflammatory macrophage responses [16], it is worth mentioning that the effect of Ptpn1 on the macrophage-IEC crosstalk is independent of direct cell-cell contact. Emerging evidence suggests that sEVs are involved in intercellular communication to regulate inflammation through reprogramming of macrophages [38–45], through transferring proteins, mRNAs, microRNAs and lipids [46–48]. In this study, we demonstrated that the conditioned medium from *Ptpn1*-KD macrophages suppresses the secretion of inflammatory cytokines and promotes barrier function of IECs. It is apparent that sEVs are primarily responsible for the beneficial effect of *Ptpn1*-KD macrophages on intestinal inflammation, because depletion of the sEVs from macrophage-conditioned medium failed to recapitulate much of the benefit conferred by *Ptpn1*-KD macrophages.

In this study, we further demonstrated differential enrichment of sEVs proteins between *Ptpn1*-KD and wild-type macrophages. Lactadherin is highly enriched in *Ptpn1*-KD macrophage sEVs and capable of promoting gut barrier function and attenuating intestinal inflammation by inhibiting NF-κB and inducing M2 polarization of macrophages. Consistently, lactadherin is known to be a component of macrophage-derived sEVs [49,50] and capable of alleviating inflammation by suppressing NF-κB activation and reprogramming macrophages [27,28,51]. Furthermore, lactadherin plays a critical role in efferocytosis [52], and the relationship between its anti-inflammatory and efferocytosis effects are largely unknown. Lactadherin neutralization in *Ptpn1*-KO mice confirmed that the anti-inflammatory effect of lactadherin was achieved through promoting efferocytic capacity of the macrophage and the clearance of apoptotic cells. It is important to dissect and evaluate relative contributions of the alleviated effects of lactadherin to the resolution of *Ptpn1*-mediated intestinal inflammation. Specifically, *Ptpn1* deficiency in the global KO mice, but not in macrophage-specific *Ptpn1* KO mice, contributes to the protection against gut barrier dysfunction and inflammation. Therefore, the isolation and characterization of intestinal macrophage and its derived sEVs in macrophage-specific *Ptpn1* KO mice will be conducted. Importantly, The effects and underlying mechanisms of sEVs from intestinal macrophage in macrophage-specific *Ptpn1* KO mice will be clarified in the future. Additionally, the mechanism by which *Ptpn1*-KD macrophages express a heightened level of lactadherin in sEVs is currently unknown. It is possible that Ptpn1 suppresses the expression of lactadherin in wild-type cells, and knockdown of *Ptpn1* releases the suppression. Although we have experimentally verified that lactadherin is a major component of the *Ptpn1*-KD macrophage sEVs responsible for the beneficial anti-inflammatory effect of sEVs, we have not ruled out the contributions of other sEVs components such as proteins, RNAs, and metabolites.

Here, we demonstrated that both macrophages and IECs preferentially take up the sEVs from *Ptpn1*-KD macrophages over those from wild-type macrophages *in vitro*. Although the differential uptake mechanism is currently unknown, engulfment of lactadherin-rich exomes from *Ptpn1*-KD macrophages by macrophages and IECs could potentially induce macrophages to the M2 phenotype and suppress NF-κB activation in IECs, respectively, leading to a collective anti-inflammatory state of the mucosal surface, which helps explain alleviation of intestinal inflammation. The reason that macrophages are indispensable in *Ptpn1*-KD sEVs-mediated protection of mice from *Salmonella* Typhimurium infection remains unknown, but M2 polarization of macrophages that are quickly recruited to the site of infection is likely to play a pivotal role in dampening infection-triggered inflammatory response.

5. Conclusion

In conclusion, the present study demonstrated that *Ptpn1* knockdown could promote alternative M2 macrophage polarization and affect macrophage-IEC interactions to maintain intestinal homeostasis. Specifically, sEVs derived from *Ptpn1*-KD macrophages is essential for the macrophage-IEC crosstalk that polarize macrophages toward M2 phenotype, thus ameliorating intestinal inflammation in a macrophage-dependent manner. Furthermore, we identified lactadherin highly expressed in sEVs produced by *Ptpn1*-KD macrophages that can serve to enhance M2 polarization and subsequently alleviate intestinal

inflammation through suppressing NF-κB activation. These findings suggest the potential of lactadherin-enriched sEVs in the treatment and prophylactics of various inflammation diseases.

Author contributions

D.H., D.L., S.H., J.P., Y.W., J.H., X.Z., and Y.P. conducted the experiment and analyzed the data. D.H. and J.W. conceived the study and wrote the manuscript. J.W. and G.Z. revised the manuscript. All authors approved the final version.

Declaration of competing interest

The author declare no conflict of interest.

Data availability

Data will be made available on request.

Acknowledgements

This work was supported by grants from the National Natural Science Foundation of China (32172750, 32125036, 31902170, and 31630074), the earmarked fund for CARS (CARS-35), the National Key Research and Development Program of China (2021YFD1300201, and 2022YFA1304201), and the 111 Project (B16044).

Appendix A. Supplementary data

Supplementary data to this article can be found online at https://doi.org/10.1016/j.redox.2022.102558.

References

[1] P. Brandtzaeg, Gate-keeper function of the intestinal epithelium, Benef. Microbes 4 (2013) 67–82.
[2] J.M. Allaire, S.M. Crowley, H.T. Law, S.Y. Chang, H.J. Ko, B.A. Vallance, The intestinal epithelium: central coordinator of mucosal immunity, Trends Immunol. 39 (2018) 677–696.
[3] M.F. Kagnoff, The intestinal epithelium is an integral component of a communications network, J. Clin. Invest. 124 (2014) 2841–2843.
[4] A.T. Soderholm, V.A. Pedicord, Intestinal epithelial cells: at the interface of the microbiota and mucosal immunity, Immunology 158 (2019) 267–280.
[5] D. Ramanan, K. Cadwell, Intrinsic defense mechanisms of the intestinal epithelium, Cell Host Microbe 19 (2016) 434–441.
[6] M.T. Abreu, Toll-like receptor signalling in the intestinal epithelium: how bacterial recognition shapes intestinal function, Nat. Rev. Immunol. 10 (2010) 131–143.
[7] C.C. Bain, A.M. Mowat, Macrophages in intestinal homeostasis and inflammation, Immunol. Rev. 260 (2014) 102–117.
[8] J. Pott, M. Hornef, Innate immune signalling at the intestinal epithelium in homeostasis and disease, EMBO Rep. 13 (2012) 684–698.
[9] P.J. Murray, Macrophage polarization, Annu. Rev. Physiol. 79 (2017) 541–566.
[10] M.R. Spalinger, A. Sayoc-Becerra, A.N. Santos, A. Shawki, V. Canale, M. Krishnan, A. Niechcial, N. Obialo, M. Scharl, J. Li, M.G. Nair, D.F. McCole, PTPN2 regulates interactions between macrophages and intestinal epithelial cells to promote intestinal barrier function, Gastroenterology 159 (2020) 1763–1777.
[11] Y.R. Na, M. Stakenborg, S.H. Seok, G. Matteoli, Macrophages in intestinal inflammation and resolution: a potential therapeutic target in IBD, Nat. Rev. Gastroenterol. Hepatol. 16 (2019) 531–543.
[12] G.T. Dodd, C.E. Xirouchaki, M. Eramo, C.A. Mitchell, Z.B. Andrews, B.A. Henry, M. A. Cowley, T. Tiganis, Intranasal targeting of hypothalamic PTP1B and TCPTP reinstates leptin and insulin sensitivity and promotes weight loss in obesity, Cell Rep. 28 (2019) 2905–2922.
[13] E. Daveri, E. Cremonini, A. Mastaloudis, S.N. Hester, S.M. Wood, A.L. Waterhouse, M. Anderson, C.G. Fraga, P.I. Oteiza, Cyanidin and delphinidin modulate inflammation and altered redox signaling improving insulin resistance in high fat-fed mice, Redox Biol. 18 (2018) 16–24.
[14] C. Rubio, M. Puerto, J.J. García-Rodríquez, V.B. Lu, I. García-Martínez, R. Alén, P. Sanmartín-Salinas, M.V. Toledo-Lobo, J. Saiz, J. Ruperez, C. Barbas, L. Menchén, F.M. Gribble, F. Reimann, L.G. Guijarro, J.M. Carrascosa, Á.M. Valverde, Impact of global PTP1B deficiency on the gut barrier permeability during NASH in mice, Mol. Metabol. 35 (2020), 100954.
[15] Á. González-Rodríguez, M.P. Valdecantos, P. Rada, A. Addante, I. Barahona, E. Rey, V. Pardo, L. Ruiz, L.M. Laiglesia, M.J. Moreno-Aliaga, C. García-Monzón, A. Sánchez, Á.M. Valverde, Dual role of protein tyrosine phosphatase 1B in the progression and reversion of non-alcoholic steatohepatitis, Mol. Metabol. 7 (2018) 132–146.
[16] P.G. Través, V. Pardo, M. Pimentel-Santillana, Á. González-Rodríguez, M. Mojena, D. Rico, Y. Montenegro, C. Calés, P. Martín-Sanz, A.M. Valverde, L. Boscá, Pivotal role of protein tyrosine phosphatase 1B (PTP1B) in the macrophage response to pro-inflammatory and anti-inflammatory challenge, Cell Death Dis. 5 (2014), e1125.
[17] X. Xu, X. Wang, Y. Guo, Y. Bai, S. He, N. Wang, Y. Lin, M. Fisher, Q. Liu, Y. Yao, Inhibition of PTP1B promotes M2 polarization via microRNA-26a/MKP1 signaling pathway in murine macrophages, Front. Immunol. 10 (2019) 1930.
[18] X. Xu, Y. Guo, J. Zhao, S. He, Y. Wang, Y. Lin, N. Wang, Q. Liu, Punicalagin, a PTP1B inhibitor, induces M2c phenotype polarization via up-regulation of HO-1 in murine macrophages, Free Radic. Biol. Med. 110 (2017) 408–420.
[19] J. Meldolesi, Exosomes and ectosomes in intercellular communication, Curr. Biol. 28 (2018) R435–R444.
[20] P.D. Robbins, A. Dorronsoro, C.N. Booker, Regulation of chronic inflammatory and immune processes by extracellular vesicles, J. Clin. Invest. 126 (2016) 1173–1180.
[21] Z. Luo, Y. Ji, H. Gao, F.C. Gomes Dos Reis, G. Bandyopadhyay, Z. Jin, C. Ly, Y. J. Chang, D. Zhang, D. Kumar, W. Ying, CRIg+ macrophages prevent gut microbial DNA-containing extracellular vesicle-induced tissue inflammation and insulin resistance, Gastroenterology 160 (2021) 863–874.
[22] T.T. Tang, B. Wang, M. Wu, Z.L. Li, Y. Feng, J.Y. Cao, D. Yin, H. Liu, R.N. Tang, S. D. Crowley, L.L. Lv, B.C. Liu, Extracellular vesicle–encapsulated IL-10 as novel nanotherapeutics against ischemic AKI, Sci. Adv. 6 (2020) eaaz0748.
[23] H. Zhao, Q. Shang, Z. Pan, Y. Bai, Z. Li, H. Zhang, Q. Zhang, C. Guo, L. Zhang, Q. Wang, Exosomes from adipose-derived stem cells attenuate adipose inflammation and obesity through polarizing M2 macrophages and beiging in white adipose tissue, Diabetes 67 (2018) 235–247.
[24] R. Kalluri, V.S. LeBleu, The biology, function, and biomedical applications of exosomes, Science 367 (2020), eaau6977.
[25] U. Erben, C. Loddenkemper, K. Doerfel, S. Spieckermann, D. Haller, M. M. Heimesaat, M. Zeitz, B. Siegmund, A.A. Kühl, A guide to histomorphological evaluation of intestinal inflammation in mouse models, Int. J. Clin. Exp. Pathol. 7 (2014) 4557–4576.
[26] D. Dasgupta, Y. Nakao, A.S. Mauer, J.M. Thompson, T.S. Sehrawat, C.Y. Liao, A. Krishnan, F. Lucien, Q. Guo, M. Liu, F. Xue, M. Fukushima, T. Katsumi, A. Bansal, M.K. Pandey, J.L. Maiers, T. DeGrado, S.H. Ibrahim, A. Revzin, K. D. Pavelko, M.A. Barry, R.J. Kaufman, H. Malhi, IRE1A stimulates hepatocyte-derived extracellular vesicles that promote inflammation in mice with steatohepatitis, Gastroenterology 159 (2020) 1487–1503.
[27] W. Ying, M. Riopel, G. Bandyopadhyay, Y. Dong, A. Birmingham, J.B. Seo, J. M. Ofrecio, J. Wollam, A. Hernandez-Carretero, W. Fu, P. Li, J.M. Olefsky, Adipose tissue macrophage-derived exosomal miRNAs can modulate in vivo and in vitro insulin sensitivity, Cell 171 (2017) 372–384.
[28] Y. Zhang, M. Brenner, W.L. Yang, P. Wang, Recombinant human MFG-E8 ameliorates colon damage in DSS-and TNBS-induced colitis in mice, Lab. Invest. 95 (2015) 480–490.
[29] Y. Lu, L. Liu, J. Pan, B. Luo, H. Zeng, Y. Shao, H. Zhang, H. Guan, D. Guo, C. Zeng, R. Zhang, X. Bai, H. Zhang, D. Cai, MFG-E8 regulated by miR-99b-5p protects against osteoarthritis by targeting chondrocyte senescence and macrophage reprogramming via the NF-κB pathway, Cell Death Dis. 12 (2021) 533.
[30] M. Bosma, M. Gerling, J. Pasto, A. Georgiadi, E. Graham, O. Shilkova, Y. Iwata, S. Almer, J. Söderman, R. Toftgard, F. Wermeling, E.A. Boström, P.A. Boström, FNDC4 acts as an anti-inflammatory factor on macrophages and improves colitis in mice, Nat. Commun. 7 (2016), 11314.
[31] B. Bernshtein, C. Curato, M. Ioannou, C.A. Thaiss, M. Gross-Vered, M. Kolesnikov, Q. Wang, E. David, L. Chappell-Maor, A. Harmelin, E. Elinav, P. Thakker, V. Papayannopoulos, S. Jung, IL-23-producing IL-10Rα-deficient gut macrophages elicit an IL-22-driven proinflammatory epithelial cell response, Sci. Immunol. 4 (2019) eaau6571.
[32] A.L. Corbin, M. Gomez-Vazquez, D.L. Berthold, M. Attar, I.C. Arnold, F.M. Powrie, S.N. Sansom, I.A. Udalova, IRF5 guides monocytes toward an inflammatory CD11c + macrophage phenotype and promotes intestinal inflammation, Sci. Immunol. 5 (2020), eaax6084.
[33] T. Castro-Dopico, A. Fleming, T.W. Dennison, J.R. Ferdinand, K. Harcourt, B. J. Stewart, Z. Cader, Z.K. Tuong, C. Jing, L.S.C. Lok, R.J. Mathews, A. Portet, A. Kaser, S. Clare, M.R. Clatworthy, GM-CSF calibrates macrophage defense and wound healing programs during intestinal infection and inflammation, Cell Rep. 32 (2020), 107857.
[34] M. Irfan Ali, P. Ketsawatsomkron, E.J. Belin de Chantelemele, J.D. Mintz, K. Muta, C. Salet, S.M. Black, M.L. Tremblay, D.J. Fulton, M.B. Marrero, D.W. Stepp, Deletion of protein tyrosine phosphatase 1b improves peripheral insulin resistance and vascular function in obese, leptin-resistant mice via reduced oxidant tone, Circ. Res. 105 (2009) 1013–1022.
[35] E.J. Belin de Chantemèle, K. Muta, J. Mintz, M.L. Tremblay, M.B. Marrero, D. J. Fulton, D.W. Stepp, Protein tyrosine phosphatase 1B, a major regulator of leptin-mediated control of cardiovascular function, Circulation 120 (2009) 753–763.
[36] D.J. Herre, J.B. Norman, R. Anderson, M.L. Tremblay, A.C. Huby, E.J. Belin de Chantemèle, Deletion of protein tyrosine phosphatase 1B (PTP1B) enhances endothelial cyclooxygenase 2 expression and protects mice from type 1 diabetes-induced endothelial dysfunction, PLoS One 10 (2015), e0126866.
[37] M. Mojena, M. Pimentel-Santillana, A. Povo-Retana, V. Fernández-García, S. González-Ramos, P. Rada, A. Tejedor, D. Rico, P. Martín-Sanz, A.M. Valverde, L. Boscá, Protection against gamma-radiation injury by protein tyrosine phosphatase 1B, Redox Biol. 17 (2018) 213–223.

[38] T.M. Bui, L.A. Mascarenhas, R. Sumagin, Extracellular vesicles regulate immune responses and cellular function in intestinal inflammation and repair, Tissue Barriers 6 (2018), e1431038.
[39] B.D. Chan, W.Y. Wong, M.M. Lee, W.C. Cho, B.K. Yee, Y.W. Kwan, W.C. Tai, Exosomes in inflammation and inflammatory disease, Proteomics 19 (2019), e1800149.
[40] M.K. McDonald, Y. Tian, R.A. Qureshi, M. Gormley, A. Ertel, R. Gao, E. Aradillas Lopez, G.M. Alexander, A. Sacan, P. Fortina, S.K. Ajit, Functional significance of macrophage-derived exosomes in inflammation and pain, Pain 155 (2014) 1527–1539.
[41] J. Guiot, M. Cambier, A. Boeckx, M. Henket, O. Nivelles, F. Gester, E. Louis, M. Malaise, F. Dequiedt, R. Louis, I. Struman, M.S. Njock, Macrophage-derived exosomes attenuate fibrosis in airway epithelial cells through delivery of antifibrotic miR-142-3p, Thorax 75 (2020) 870–881.
[42] H. Higuchi, N. Yamakawa, K.I. Imadome, T. Yahata, R. Kotaki, J. Ogata, M. Kakizaki, K. Fujita, J. Lu, K. Yokoyama, K. Okuyama, A. Sato, M. Takamatsu, N. Kurosaki, S.M. Alba, A. Azhim, R. Horie, T. Watanabe, T. Kitamura, K. Ando, T. Kashiwagi, T. Matsui, A. Okamoto, H. Handa, M. Kuroda, N. Nakamura, A. Kotani, Role of exosomes as a proinflammatory mediator in the development of EBV-associated lymphoma, Blood 131 (2018) 2552–2567.
[43] J. Lan, L. Sun, F. Xu, L. Liu, F. Hu, D. Song, Z. Hou, W. Wu, X. Luo, J. Wang, X. Yuan, J. Hu, G. Wang, M2 macrophage-derived exosomes promote cell migration and invasion in colon cancer, Cancer Res. 79 (2019) 146–158.
[44] K. Jiang, J. Yang, S. Guo, G. Zhao, H. Wu, G. Deng, Peripheral circulating exosome-mediated delivery of miR-155 as a novel mechanism for acute lung inflammation, Mol. Ther. 27 (2019) 1758–1771.
[45] Y. Pan, X. Hui, R.L.C. Hoo, D. Ye, C.Y.C. Chan, T. Feng, Y. Wang, K.S.L. Lam, A. Xu, Adipocyte-secreted exosomal microRNA-34a inhibits M2 macrophage polarization to promote obesity-induced adipose inflammation, J. Clin. Invest. 129 (2019) 834–849.
[46] H. Zhang, L. Wang, C. Li, Y. Yu, Y. Yi, J. Wang, D. Chen, Exosome-induced regulation in inflammatory bowel disease, Front. Immunol. 10 (2019) 1464.
[47] H. Choi, Y. Kim, A. Mirzaaghasi, J. Heo, Y.N. Kim, J.H. Shin, S. Kim, N.H. Kim, E. S. Cho, J. In Yook, T.H. Yoo, E. Song, P. Kim, E.C. Shin, K. Chung, K. Choi, C. Choi, Exosome-based delivery of super-repressor IκBα relieves sepsis-associated organ damage and mortality, Sci. Adv. 6 (2020), eaaz6980.
[48] G. Szabo, Exosomes and MicroRNA-223 at the intersection of inflammation and fibrosis in NAFLD, Hepatology 74 (2021) 5–8.
[49] L. Bouchareychas, P. Duong, S. Covarrubias, E. Alsop, T.A. Phu, A. Chung, M. Gomes, D. Wong, B. Meechoovet, A. Capili, R. Yamamoto, H. Nakauchi, M. T. McManus, S. Carpenter, K. Van Keuren-Jensen, R.L. Raffai, Macrophage exosomes resolve atherosclerosis by regulating hematopoiesis and inflammation via microRNA cargo, Cell Rep. 32 (2020), 107881.
[50] Y. Yue, C. Wang, C. Benedict, G. Huang, M. Truongcao, R. Roy, M. Cimini, V.N. S. Garikipati, Z. Cheng, W.J. Koch, R. Kishore, Interleukin-10 deficiency alters endothelial progenitor cell-derived exosome reparative effect on myocardial repair via integrin-linked kinase enrichment, Circ. Res. 126 (2020) 315–329.
[51] M.J. Brissette, S. Lepage, A.S. Lamonde, I. Sirois, J. Groleau, L.P. Laurin, J. F. Cailhier, MFG-E8 released by apoptotic endothelial cells triggers anti-inflammatory macrophage reprogramming, PLoS One 7 (2012), e36368.
[52] A. Das, S. Ghatak, M. Sinha, S. Chaffee, N.S. Ahmed, N.L. Parinandi, E.S. Wohleb, J. F. Sheridan, C.K. Sen, S. Roy, Correction of MFG-E8 resolves inflammation and promotes cutaneous wound healing in diabetes, J. Immunol. 196 (2016) 5089–5100.